Adaptive laboratory evolution of Lipomyces starkeyi for high production of lignin derivative alcohol and lipids with comparative untargeted metabolomics-based analysis

Putra, Filemon Jalu Nusantara
Kahar, Prihardi
Kondo, Akihiko
Ogino, Chiaki

(Citation)
Microbial Cell Factories,23(1):270

(Issue Date)
2024-10-08

(Resource Type)
journal article

(Version)
Version of Record

(URL)
https://hdl.handle.net/20.500.14094/0100491802

Microbial Cell Factories

RESEARCH Open Access

Adaptive laboratory evolution of *Lipomyces starkeyi* for high production of lignin derivative alcohol and lipids with comparative untargeted metabolomics-based analysis

Filemon Jalu Nusantara Putra[1], Prihardi Kahar[1], Akihiko Kondo[2] and Chiaki Ogino[1*]

Abstract

Background Adaptive laboratory evolution (ALE) is an impactful technique for cultivating microorganisms to adapt to specific environmental circumstances or substrates through iterative growth and selection. This study utilized an adaptive laboratory evolution method on *Lipomyces starkeyi* for high tolerance in producing lignin derivative alcohols and lipids from syringaldehyde. Afterward, untargeted metabolomics analysis was employed to find the key metabolites that play important roles in the better performance of evolved strains compared to the wild type. Lignin, a prominent constituent of plant biomass, is a favorable source material for the manufacture of biofuel and lipids. Nevertheless, the effective transformation of chemicals produced from lignin into products with high economic worth continues to be a difficult task.

Results In this study, we exposed *L. starkeyi* to a series of flask passaging experiments while applying selective pressure to facilitate its adaptation to syringaldehyde, a specific type of lignin monomeric aldehyde. Using ALE, we successfully developed a new strain, DALE-22, which can synthesize syringyl alcohol up to 18.74 mM from 22.28 mM syringaldehyde with 41.9% lipid accumulation. In addition, a comprehensive examination of untargeted metabolomics identified six specific crucial metabolites linked to the improved tolerance of the evolved strain in the utilization of syringaldehyde, including 2-aminobutyric acid, allantoin, 4-hydroxyphenethyl alcohol, 2-aminoethanol, tryptophan, and 5-aminovaleric acid.

Conclusion The results of our study reveal how *L. starkeyi* adapts to using substrates produced from lignin. These findings offer important information for developing strategies to improve the process of converting lignin into valuable products for sustainable biorefinery applications.

Keywords Oleaginous yeast, Biochemical production, Lignin valorization, Microbial lipid synthesis, Metabolomics, Comparative analysis

*Correspondence:
Chiaki Ogino
ochiaki@port.kobe-u.ac.jp
[1]Department of Chemical Science and Engineering, Graduate School of Engineering, Kobe University, 1-1 Rokkodaicho, Nada-Ku, Kobe 657-8501, Japan
[2]Graduate School of Science, Technology and Innovation, Kobe University, 1-1 Rokkodaicho, Nada-Ku, Kobe 657-8501, Japan

Introduction

Lignocellulosic biomass is a highly promising and renewable resource that may be used to produce biofuels and biochemicals in a sustainable manner. It has the ability to address the increasing energy and environmental issues faced by the world [1–3]. Lignin, a complex and plentiful polymer, is of special interest among its components because of its potential as a raw material for producing biofuels. Nevertheless, the process of extracting value from lignin is still a significant obstacle, mainly because of its resistant characteristics and the intricate chemical reactions required to break it down [4–6]. Recently, there has been a strong focus on utilizing monomeric aldehydes produced from lignin as material substrates for producing valuable bioproducts, such as lignin monomer alcohols and lipids. *Lipomyces starkeyi*, a non-traditional yeast species that can produce a large amount of oil, is a highly attractive choice for this application. It is particularly notable for its exceptional capacity to break down various carbon sources, including specific aldehydes generated from lignin [7, 8]. Nevertheless, in order to obtain substantial amounts of desired substances from lignin monomers utilizing *L. starkeyi*, it is necessary to overcome certain challenges related to its fundamental biological processes and control mechanisms. Adaptive Laboratory Evolution (ALE) is a highly effective method for cultivating microorganisms to adjust to certain environmental conditions or substrates by repeatedly growing and selecting them [9–12]. The process of ALE involves exposing wild-type of *L. starkeyi* (WT) to progressively higher concentrations of specific lignin derivative aldehydes, such as syringaldehyde. This method enables the development of desired characteristics in the organism, including improved utilization of substrates, increased metabolic efficiency, and enhanced synthesis of products. Within the framework of lignin valorization, ALE shows significant potential for enhancing microbial strains to achieve more efficient conversion of lignin-derived aldehydes into desired bioproducts, such as syringyl alcohol and lipids.

The objective of this work is to investigate the capacity of ALE as a method to improve the synthesis of lignin-derived alcohols and lipids from syringaldehyde using *L. starkeyi*. We aim to understand the adaptive mechanisms that lead to improved use of resources and production of substances in *L. starkeyi* by conducting systematic evolution experiments and doing detailed analyses of its characteristics and metabolism (Fig. 1). In addition, untargeted metabolomics analysis was used to discover significant compounds that may have a crucial function in the metabolic reconfiguration of the evolved strain. In this study, we assess the efficiency of evolved strains in terms of productivity, yield, and substrate specificity. Our ultimate goal is to create durable microbial platforms that may be used for the economical and sustainable conversion of lignocellulosic biomass in biorefining processes. It will leverage the adaptability of microbial systems through ALE and advanced metabolomics techniques.

Materials and methods

Mutants development by serial flask cultivation

The syringaldehyde used in this study was obtained from Sigma Aldrich Co. LLC. The source of syringyl alcohol was Thermo Fisher Scientific Inc. (USA). Methanol and chloroform were purchased from Nacalai Tesque (Japan). An oleaginous yeast, *Lipomyces starkeyi* D35 (NBRC10381) was used as a model organism. The National Institute of Technology and Evaluation Biological Resource Center in Japan provided the organism. The yeast was preserved in a glycerol solution with a concentration of 30% (w w^{-1}) at a temperature of -80 °C. After that, the yeast was prepared by inoculating it into a Potato Dextrose Agar (PDA) medium. Subsequently, a single colony was moved to a YMPG (Yeast Malt Peptone

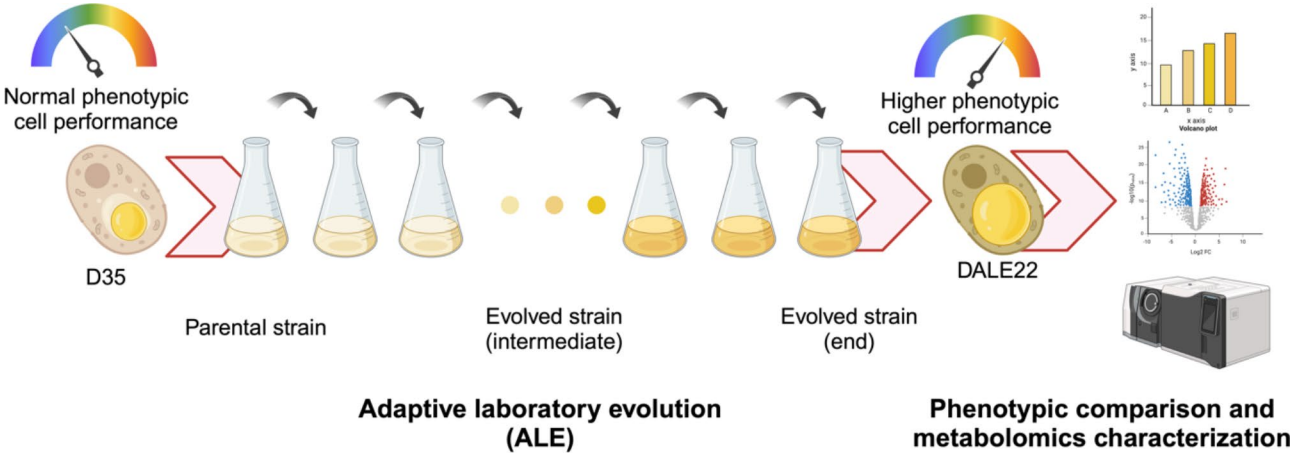

Fig. 1 Overview of flask scale adaptive laboratory evolution and phenotypic comparison with untargeted metabolomics characterization

Glucose) agar medium consisting of 3 g L^{-1} malt extract, 3 g L^{-1} yeast extract, 5 g L^{-1} peptone, 10 g L^{-1} glucose, and 20 g L^{-1} agar. The incubation period lasted for 48 h at a temperature of 30 °C. To initiate fermentation, a solitary colony was placed into a 12 mL liquid medium called YMPG-50. This medium consisted of 3 g L^{-1} malt extract, 3 g L^{-1} yeast extract, 5 g L^{-1} peptone, and 50 g L^{-1} glucose. The transfer was made into a 100 mL flask, and the pre-culture was incubated overnight. Afterward, the pre-culture was moved to a fresh 12 mL YMPG-50 medium with 8 mM syringaldehyde as the primary culture in a 100 mL flask. The inoculum concentration for the fermentation in the primary culture was adjusted to 1 unit (OD_{600}). The flask was incubated at 190 rpm and 30 °C in a BioShaker BR-43FH MR orbital incubator shaker (Taitec Corp., Japan). The strain was developed by repeatedly transferring it in shaking flasks using YMPG-50 media with a controlled increase in syringaldehyde. The experiment began with a single unit (OD_{600}) of the wild-type *L. starkeyi* D35 strain, which was grown in 12 mL of YMPG-50 media supplemented with 8 mM syringaldehyde. The optical density (OD) was regularly monitored every 24 h to track the growth of the cells. Once the cell growth exceeds 30 units, the cells are transferred to a fresh medium with a comparable quantity of syringaldehyde. The cells were moved to a greater concentration of syringaldehyde only when the growth rate reached 0.62 units (OD_{600}) h^{-1}. An addition of 2 mM of syringaldehyde was used in every increment transfer with an initial inoculum concentration of 1 unit from the previous fermentation. Afterward, the cell was transferred into 30% (w w^{-1}) glycerol with the selective concentration of syringaldehyde from fermentation and stored at -80 °C until further analysis. At the end of the adaptation, a screening of cell growth (DCW) was performed to choose the most well-developed cells by first steaking into YMPG-50 agar with a selective concentration of syringaldehyde, then colonies subjected to fermentation.

Measurement of cell growth

A gravimetric approach was utilized to measure the DCW (Dry Cell Weight), which involved using 0.5 mL of fermentation samples. The cell was isolated using centrifugation for 5 min at a force of 14,000 × g. Immediately following, the cells were cleaned with sterile water and subjected to lyophilization overnight to remove all water content. The lyophilization process was conducted using a freeze dryer called Freeze Dry, FreeZone model manufactured by Labconco, United States. Subsequently, the determination of DCW was conducted by considering the weight of the dehydrated cells.

Glucose consumption measurement by HPLC-RID

Glucose concentration was measured during fermentation using an HPLC (high-performance liquid chromatography) system from Shimadzu, Japan, coupled to a RI (refractive index) detector. The system was outfitted with a column of ICSep Coregel-87 H, which had a diameter of 7.8 mm and a length of 300 mm. The column was provided by Transgenomic. Before analysis, the samples were prepared by centrifuging at a force of 14,000 × g for 5 min, then filtering the supernatant through a 0.22 mm filter. The analysis required injecting a sample amount of 20 µL while keeping the column oven at 80 °C. The analysis used a mobile phase of 5 mM H_2SO_4, with a flow rate of 0.6 mL min^{-1} [13].

Lignin quantification by HPLC-UV/Vis

The quantification of lignin derivatives was conducted using an HPLC-20AB system manufactured by Shimadzu, Japan. The system was equipped with an ultraviolet-visible spectroscopy (UV/Vis) detector model SPD-20 A. The analysis employed a C18 column (250 mm length x 4.6 mm, 5 µm particle size) obtained from Supelco Ascentis (Merck KGaA, Darmstadt, Germany). The supernatant samples were prepared for analysis by subjecting them to centrifugation for 5 min at 14,000 × g, then continued by filtration using a 0.22 mm filter. 10 µL of sample was injected for each measurement, and the column oven was kept at a constant temperature of 30 °C for 45 min. The mobile phase consisted of a blend of methanol and water (HPLC grade) in a volumetric ratio of 18:82, with the addition of 0.2% acetic acid (v v^{-1}). This combination passed the column at a flow rate of 1 mL min^{-1}, and the analytes were measured at a wavelength of 280 nm [7].

Lipid measurement

The measurement of lipid production was conducted using a gravimetric method, following the procedure outlined by Folch [14, 15]. 20 mg of freeze-dried samples were measured and placed into a 2 mL micro vial with an O-ring cap closure (Watson, Japan). To enhance the extraction process, zirconia balls were added to the microvial. A 1.5 mL volume of extraction solvent, composed of a mixture of chloroform and methanol in a ratio of 2:1 (v v^{-1}), was utilized to extract the lipids. The cells were subsequently pulverized at a speed of 1500 rpm for 15 min using a Master Neo pulverizer manufactured by Bio-Medical Science in Japan. Subsequently, the cells were centrifugated at a force of 14,000 × g for 5 min. Afterward, the cell pellets were cleaned with sterile water. The cells were dried at 60 °C until they reached a stable weight. The lipid content was assessed by measuring the weight difference before and after drying and then expressed as a percentage of DCW.

Fatty acid profiling by GC/MS

The lipids from the lyophilized samples were converted into fatty acid methyl esters (FAMEs) using a transesterification technique described in the FAMEs mixture kit (Nacalai Tesque, Japan). The resulting FAMEs were dissolved in hexane and analyzed by GC/MS (gas chromatography-mass spectrometry) QP-2010 (Shimadzu, Japan). A C8:0 (caprylic acid) internal standard was included in the sample as a reference. The examination was conducted utilizing a capillary gas chromatography (GC) column DB-23 (0.25 mm internal diameter, 60 m length, 0.25 mm thickness) manufactured by Agilent. The carrier gas employed was helium. A 1 µL sample injection volume was used, and the analysis was performed using split injection with an inlet temperature of 250 °C. The oven program began at 50 °C for 1 min, then increased at a rate of 25 °C min^{-1} up to 175 °C. After that, it further increased to 230 °C at a rate of 4 °C min^{-1}, and this temperature was kept for 6 min. The MS detector was set to 250 °C and utilized the scan mode to cover the range of 40 to 500 m z^{-1}. The fatty acids were identified and quantified by matching their m z^{-1} and retention times (rt) configuration with a standard fatty acid mix, SUPELCO 37 FAME mix (Sigma–Aldrich) [14].

Fast filtration, extraction, and derivatization of intracellular metabolites

The process of collecting samples for investigation of intracellular metabolome was carried out using the rapid quenching filtering method. The cells were harvested during the logarithmic phase after 24 h of growth, with an optical density (OD_{600}) of 5 units. The filtration was performed using a 0.45 µm pore size nylon membrane filter with a diameter of 25 mm, manufactured by Millipore, United States. The cells were immediately cooled in liquid nitrogen to halt metabolic activity and then stored at a temperature of -80 °C before extraction. The metabolites were extracted using 3 mL of extraction solution (methanol: ultra-pure water: chloroform; 5:2:2 v v-1 ratio), which included 10 µg L^{-1} of ribitol as an internal standard. The extraction process was carried out under thawing incubation conditions. The thawing process involved subjecting the sample to a temperature of -80 °C for 1 h, followed by a temperature of -30 °C for 30 min, repeated three times. Subsequently, 1 mL of the liquid remaining after centrifugation was moved to a different small tube and combined with 200 µL of highly purified water. Afterward, the sample was subjected to centrifugation at 10,000 × g for 10 min at a temperature of 4 °C. Subsequently, 950 µL of the upper phase was collected. The sample was concentrated using a centrifugal dryer for 2 h and then freeze-dried in the freeze-drier overnight. The process of derivatization, involving oximation and trimethylsilylation, was carried out before conducting GC/MS analysis. The initial derivatization process was the addition of methoxiamine hydrochloride (100 µL, 20 mg ml^{-1} in pyridine) and incubation at 30 °C for 90 min. The second derivatization agent, MSTFA (N-methyl-N-(trimethylsilyl) trifluoroacetamide) [16], was added to the mixture in a volume of 50 µL. The mixture was then incubated at 37 °C for 30 min.

Analysis of intracellular untargeted metabolites by GC/MS

Gas chromatography-mass spectrometry (GC/MS) was used to perform an untargeted investigation of intracellular metabolites. The GC/MS QP2020 and AOC-20i autosampler, manufactured by Shimadzu in Kyoto, Japan, is fitted with a 0.25 mm × 30 m × 0.25 µm inert Cap 5 MS/NP column, provided by GL Science Inc. in Tokyo, Japan. The modified sample (1 µL) was analyzed using GC/MS in split mode with an injection temperature of 230 °C. The carrier gas utilized was helium, flowing at a rate of 1.12 mL min^{-1}, resulting in a linear velocity of 39 cm s^{-1}. The column was first held at a temperature of 80 °C for 2 min. Subsequently, the temperature was raised at a rate of 15 °C min^{-1} until it reached 330 °C. At this point, the temperature was maintained for 6 min. The transfer line and ion source in the mass spectrometry section were maintained at temperatures of 250 and 200 °C, respectively. Electron ionization (EI) produced ions at a 0.93 kilovolts (kV) voltage. The spectra were captured at a rate of 10,000 units per second across the mass range of m z^{-1} (mass to charge ratio) 85–500. The retention index calibration was performed by injecting the terminal alkane standard mixture (C8–C40) for tentative identification.

Metabolome data and multivariate analysis

The data generated from gas chromatography-mass spectrometry (GC/MS) were exported as ANDI files (cdf) using Shimadzu GCMS Solution software (Kyoto, Japan). Subsequently, the data was transformed into ABF format via Reifycs Analysis Base File software. MS-DIAL v. 3.9.22 (Riken, Kanagawa, Japan) was used to correct the baseline, identify the peaks, and align the retention times of the peaks. Subsequently, the identified peaks were labeled using the retention time and mass spectrometry data, referring to the publicly available metabolite library, GL-Science database, shared by RIKEN. The data patterns were analyzed using multivariate analysis with MetaboAnalyst 6.0 (https://www.metaboanalyst.ca) for PCA (Principal Component Analysis) without any data transformation. The analysis focused on identifying differences and similarities among the data. The relative intensity of each metabolite was adjusted by comparing it to the internal standard (ribitol) as an explanatory variable. The data was rescaled automatically to minimize the obscuring impact of all metabolites.

Results and discussion

Evolved phenotypic changes

We utilized adaptive laboratory evolution (ALE) to enhance the bioconversion efficiency of *L. starkeyi* in converting lignin aldehyde into useful lignin alcohol and lipids. This was achieved by continuously alternating the medium substrates. The original strain of *L. starkeyi* D35 (NBRC10381) was chosen as the parental strain because this strain has been previously used as a platform to convert biomass-derived lignin aldehydes into lignin alcohols [8, 17]. The strain development in shake flasks on YMPG-50 medium by gradually adding syringaldehyde. The initial inoculum size utilized in fermentation was 1 (OD_{600}). The optical density of the cells was regularly tested. After it reached a value of 30 units, the cells were transferred to a new medium containing a comparable concentration of syringaldehyde. Syringaldehyde was introduced into the medium only after the growth rate reached 0.62 (OD_{600}) h^{-1}, at a higher concentration. ALE of *L. starkeyi* was terminated after 20 transfers conducted over a span of 81 days, as no additional enhancement in growth was detected after 20 transfers. At this stage, the cell could simultaneously synthesize syringyl alcohol and lipids from syringaldehyde, which was achieved at a concentration of 22 mM. Following the completion of the adaptation, cell growth (DCW) screening was conducted to choose the best-developed cells. After screening, the single isolated colony showed the highest cell growth (Fig. S2). The chosen evolved strain was labeled as DALE-22. This colony was chosen for further investigation.

When DALE 22 and WT (D35) were fermented with 22 mM syringaldehyde, DALE 22 demonstrated superior performance compared to WT in all aspects (Table 1). Figure 2 demonstrates that DALE 22 effectively generated 18.74 mM of syringyl alcohol from 22.28 mM of syringaldehyde throughout a 96 h period, utilizing a lipid content of 30%. Conversely, the original strain of parents was unable to thrive and lost its capacity to transform syringaldehyde into syringyl alcohol. A high concentration of syringaldehyde in the medium can cause significant cell damage to the WT strain, leading to a loss of conversion ability and impaired growth, even at the early stages of fermentation. Syringaldehyde, a type of lignin monomeric molecule, is recognized as an inhibitor for certain living organisms [18]. Utilizing the process of adaptive evolution, known as ALE, to strengthen the inherent potential.

Table 1 Dry cell weight and lipid production of *L. Starkeyi* in 22 mM syringaldehyde[a]

Strain	Time	Initial DCW	Final DCW	Final lipid content	Lipid titer
	(h)	(g L^{-1})	(g L^{-1})	(w w^{-1}%)	(g L^{-1})
WT	0	0.3 ± 0.1	11.4 ± 0.9	32.0 ± 0.0	3.6 ± 0.0
	96	0.6 ± 0.0	0.8 ± 0.0	0.0 ± 0.0	0.0 ± 0.0
DALE-22	0	0.4 ± 0.1	11.7 ± 0.7	33.0 ± 4.6	3.8 ± 0.0
	96	0.8 ± 0.2	12.9 ± 0.7	41.9 ± 4.6	5.4 ± 0.0

[a]The data displayed represents the average of three biological replicate samples, with error bars showing the standard deviation from the mean

Fermentation profile of evolved strain in mild syringaldehyde

To examine significant metabolites that may have a crucial impact on the evolved strain in comparison to the parental strain, we conducted fermentation using a lower dose of syringaldehyde (4 mM), which is conducive to the growth of the parental strain. Later on, we investigated the intracellular metabolite utilizing untargeted metabolomics analysis with GC/MS equipment. Cells have a high level of complexity, with numerous regulatory processes coinciding within a brief timeframe, particularly concerning metabolites. The fermentation should be maintained under consistent conditions to acquire the precise role of regulation in cells [19].

According to the fermentation profiling results (Fig. 3), the growth patterns of the evolved and wild-type strains appear to be similar. Nevertheless, the evolved strains exhibited a greater cell production of 18.2 g L^{-1} compared to the original strains, which produced 17.1 g L^{-1} (Table 2). The growth rate at the logarithmic state was 0.40 DCW h^{-1} L^{-1} for the evolved strains and 0.31 DCW h^{-1} L^{-1} for the parental strains. The data indicate that DALE-22 exhibits tolerance compared to the wild-type, even under similar fermentation conditions. After 24 h of fermentation, the syringaldehyde was completely used up, and the evolved strains and parental strains successfully generated syringyl alcohol at concentrations of 3.19 mM and 3.18 mM, respectively. Syringyl alcohol is a valuable chemical in lignin and is frequently employed in research on lignin models. The most recent study, focusing on syringyl alcohol, demonstrates its remarkable catalytic efficacy when used as a probe in carbon nanotubes [20]. DALE-22 exhibited a more outstanding lipid content in comparison to the parental strain, as shown in Fig. 3c. *L. starkeyi* can convert various monomeric aldehydes into valuable lignin monomeric alcohols via the intracellular AKR (aldehyde-ketone reductase) enzyme. AKR catalyzes the conversion of a lignin monomeric aldehyde to alcohol, resulting in the production of one additional $NAD(P)^+$ molecule. This $NAD(P)^+$ molecule can potentially be utilized in converting malate to pyruvate by releasing cytosolic NAD(P)H. Pyruvate is potentially associated with the Krebs cycle, which is essential for cellular development and the generation of triacylglyceride (TAG) lipids [7]. A higher level of adaptability in DALE-22 positively impacted the generation of by-products, such as lipids.

Figure 4 displays the fatty acid profile that results from fermentation processes in 4 mM of syringaldehyde.

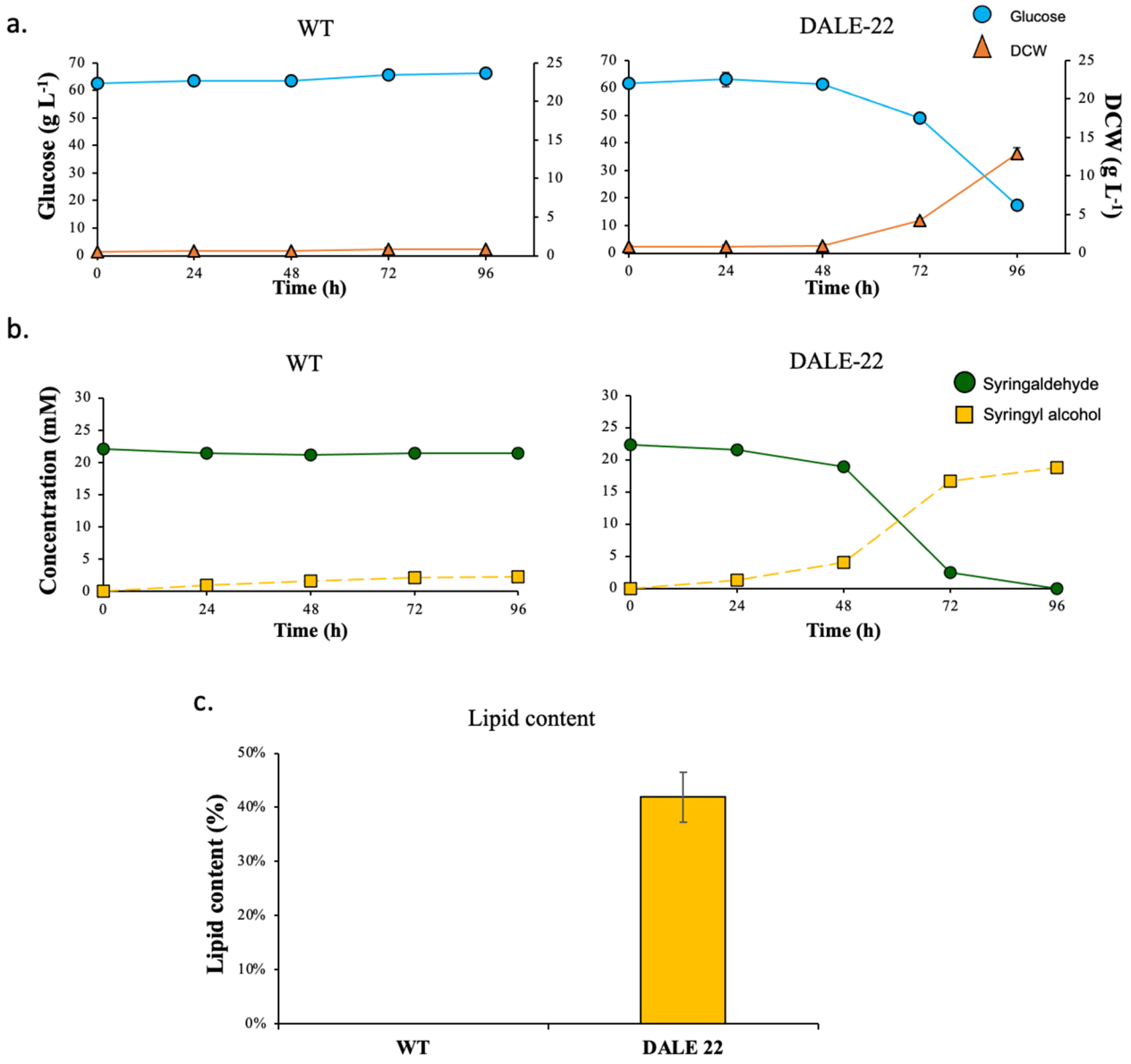

Fig. 2 Fermentation profile of DALE-22 and WT in the 22 mM concentration of syringaldehyde. (**a**) Growth curve and glucose consumption. (**b**) Syringaldehyde conversion and syringyl alcohol production. (**c**) Lipid content. The data displayed represents the average of three biological replicate samples, with error bars showing the standard deviation from the mean

Long-chain fatty acids (LCFAs) such as C18:1 (oleic acid) and C16:0 (palmitic acid) were the predominant fatty acid composition of the lipids (Fig. 4a), which is similar to the common compositions of many oils such as vegetable oils [21]. Notably, oleic acid was the predominant fatty acid in both fermentations, making up more than 40% of the total fatty acids. Palmitic acid constituted approximately 30% o the total fatty acids in WT. On the other hand, DALE-22 is significantly lower. Due to the high concentration of oleic acid, DALE-22 may play a significant role in the industrial manufacture of biodiesel in the future. *L. starkeyi* species showed the most oleic acid synthesis among the oleaginous yeast strains [14, 22], yet DALE-22 was even able to produce higher than its wild-type strain.

In the major fatty acids, C18:2 (linolelaidic acid), C18:1 (oleic acid), and C18:0 (stearic acid) were found to be higher in the DALE-22. Nevertheless, fatty acids C16:1 and C16:0 (oleic acid). Minor fatty acids, including C14:0 (myristic acid) and C15:0 (pentadecanoic acid) (Fig. 4b), exhibit an increase in WT. By obstructing the synthesis of fatty acids, inhibitors such as phenolic substances may impact the increase of LCFAs in the microbes. It may inhibit the prolongation and induction steps of fatty acid synthesis, respectively, by targeting key enzymes

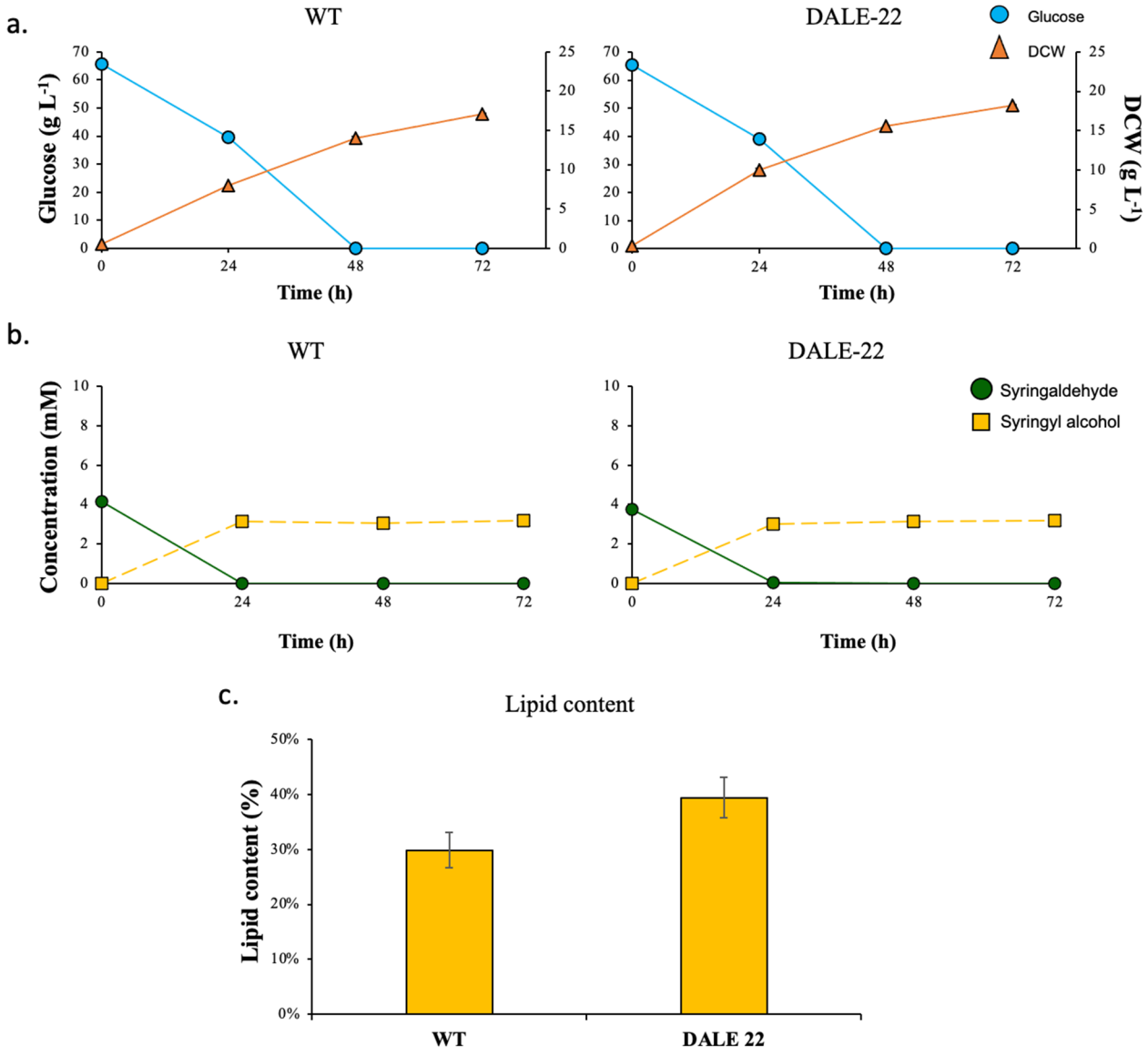

Fig. 3 Fermentation profile of DALE-22 and WT in the 4 mM concentration of syringaldehyde. (**a**) Growth curve and glucose consumption. (**b**) Syringaldehyde conversion and syringyl alcohol production. (**c**) Lipid content. The data displayed represents the average of three biological replicate samples, with error bars showing the standard deviation from the mean

Table 2 Dry cell weight and lipid production of *L. Starkeyi* in 4 mM syringaldehyde.[a]

Strain	Time	Initial DCW	Final DCW	Final lipid content	Lipid titer
	(h)	(g L^{-1})	(g L^{-1})	(w w^{-1}%)	(g L^{-1})
WT	72	0.5 ± 0.1	17.1 ± 0.1	29.9 ± 3.2	5.1 ± 0.0
DALE-22	72	0.4 ± 0.0	18.2 ± 0.1	39.4 ± 3.7	7.2 ± 0.0

[a]The data displayed represents the average of three biological replicate samples, with error bars showing the standard deviation from the mean

like acetyl-CoA carboxylase or β-ketoacyl carrier protein (ACP) synthases (KSs), which would reduce the systematic production of LCFAs and consequent imbalance in the fatty acid profile [23, 24]. However, this phenomenon can serve as a helpful method for regulating the production of lipids that include a significant proportion of specific long-chain fatty acids, such as oleic acid, for various biotechnological purposes.

Comparative untargeted metabolomics analysis of evolved strain

Untargeted GC/MS analysis was performed to determine the intracellular metabolites present throughout the logarithmic phase of both the DALE-22 (evolved strain) and WT (parental strain). Following the completion of identification, a total of 73 metabolites from various categories, including amino acids, organic acids, nucleoside

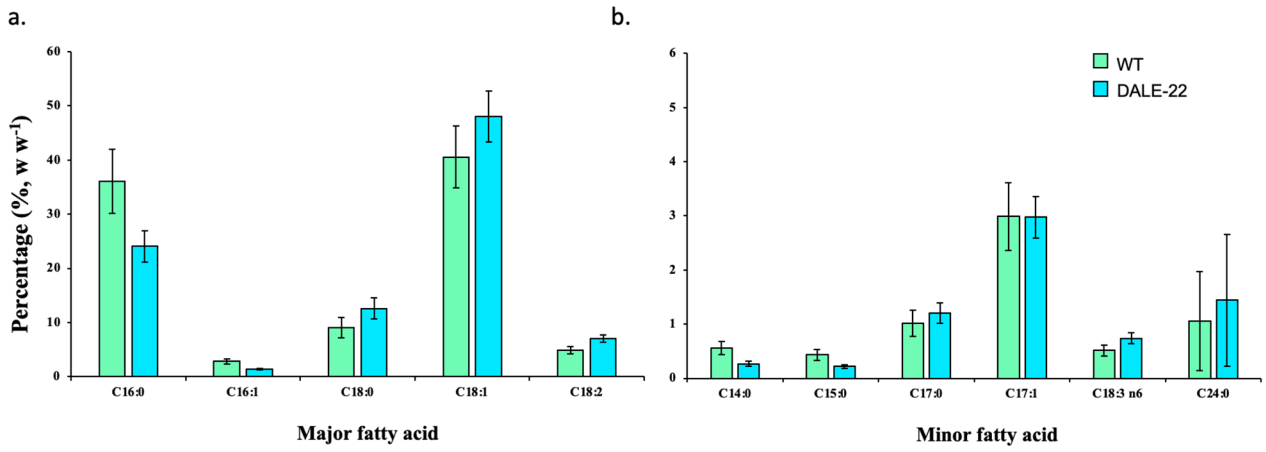

Fig. 4 Profiles of fatty acids produced during the fermentation of DALE-22 and WT in 4 mM concentration of syringaldehyde. (**a**) Major fatty acid percentage in lipids. (**b**) Minor fatty acid percentage in lipids. The data displayed represents the average of three biological replicate samples, with error bars showing the standard deviation from the mean

phosphate, nucleosides, sugars, sugar phosphate, and other chemicals, were successfully annotated in both DALE-22 and WT samples (Fig. S3). Ribitol was used as an internal standard, each metabolite's relative intensity was calculated based on it. Ribitol was selected as an internal standard for the analysis since it is not naturally found in any biological materials, including *L. starkeyi* cells. Additionally, it is known to be a chemically stable compound in the extraction solvent until the analysis takes place [16]. A multivariate analysis was conducted on a total of 73 metabolites. The Principal Component Analysis (PCA) of the GC/MS dataset revealed that two principal components (PC) accounted for 79.8% of the overall variation (Fig. 5). Given that glucose consumption, growth, lipid generation, and bioconversion of lignin monomers are most vigorous during the logarithmic phase, studying and tracking the metabolite levels during this phase would provide the most accurate representation of the cells phenotypic state during bioconversion. A comprehensive principal component analysis (PCA) was performed specifically for the logarithmic phase. The analysis revealed that DALE-22 and WT were distinctly differentiated based on PC 1, which explained 61.9% of the overall variability (Fig. 5). These data may suggest a correlation between the conversion ability and tolerance phenotype of the two strains. DALE-22 has distinct characteristics in terms of its growth, bioconversion ability, and lipid synthesis. The heatmap analysis additionally indicates the regulation of distinct metabolites (Fig. 5c).

To provide more specific information, differential analysis was employed to further examine the disparities in the metabolites. Figure 6 shows the volcano plot that depicted the metabolites that exhibited a statistically significant increase in expression [25]. When comparing DALE-22 with WT, metabolites with p-values lower than 0.05 were indicated above the line. The dots were positioned above the threshold of minus log10 t-test p-values of 1.746. The log2 fold change values were employed to quantify the extent of changes in metabolite quantities. A log2 fold change of 1 indicates that the metabolite on the right side, shown with a red dot, has doubled in abundance in DALE-22 compared to the subsequent measurement. Conversely, a log2 fold change of 2 signifies that the metabolite on the right side, also marked with a red dot, is 4 times greater. In contrast, negative values of log2 fold change indicate a reduction in metabolites in DALE-22 compared to a subsequent measurement. The representation consisted of purple dots. Figure 7 shows that 2-aminobutyric acid (GABA) was the predominant component detected in DALE-22, surpassing the levels found in the parental strain. GABA, a metabolite, exhibits a protective role in microbes under stressful circumstances and it is produced through the decarboxylation of glutamate, a reaction catalyzed by the enzyme glutamate decarboxylase (GAD) [26]. The increased tolerance refers to the yeast's improved ability to survive and maintain functionality under stress conditions. GABA may help the cell manage stress by acting as an osmoprotectant, stabilizing cellular structures, or modulating stress-related signaling pathways. A cell that exhibits enhanced GABA production in response to stress may possess increased tolerance [27]. Furthermore, allantoin, which is abundantly present in the DALE-22, is recognized for its role as an antioxidant that protects against oxidative stress. Allantoin is a secondary product resulting from the process of purine catabolism, which involves the breakdown of purine nucleotides. Although it does not directly participate in the stress response, this metabolite exhibits strong antioxidant properties. Cells that possess elevated amounts of allantoin may exhibit enhanced resistance to oxidative

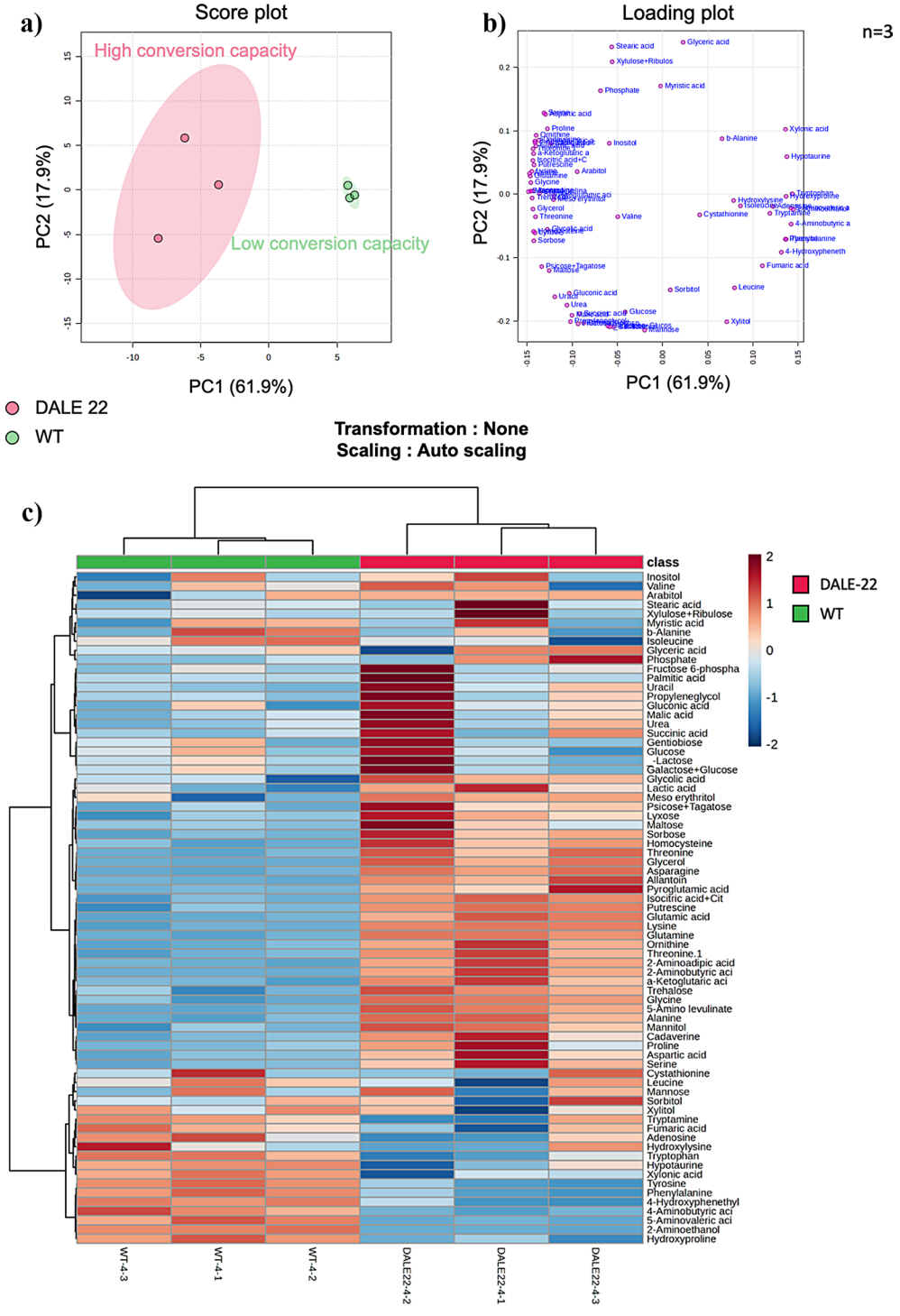

Fig. 5 GC/MS metabolomics profiles of intracellular DALE-22 and WT under 4 mM syringaldehyde. (**a**) Principle Component Analysis (PCA) score plot of DALE-22 and WT. Red points indicate DALE-22, and green points indicate WT. (**b**) PCA loading plot of the metabolites obtained from GC–MS profiling of DALE-22 and WT. (**c**) Heatmap analysis of untargeted metabolites detected during the logarithmic phase in the presence of 4 mM syringaldehyde

stress [28]. In contrast, the parental strain exhibited higher levels of 2-amino ethanol (ethanolamine) and 4-hydrophenethyl alcohol compared to DALE-22. These metabolites can help maintain osmotic equilibrium or function as signaling molecules. Cells with enhanced capacity to use these chemicals may exhibit greater resistance to specific environmental stressors [29–31]. In addition, the levels of tryptophan and 5-amino valeric acid were reduced in the DALE-22. Tryptophan is a crucial amino acid utilized in the process of protein

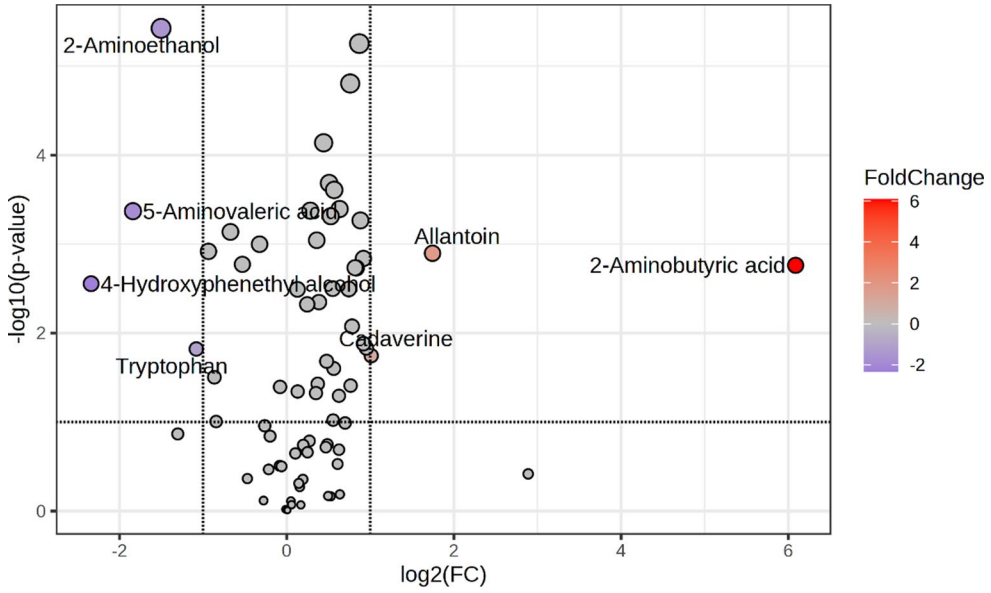

Fig. 6 The volcano plots illustrate the distinct metabolites in DALE-22 in comparison to WT. The x-axis represents the binary logarithm of fold changes, while the y-axis represents the negative common logarithm of the *p*-value derived from pairwise student t-tests

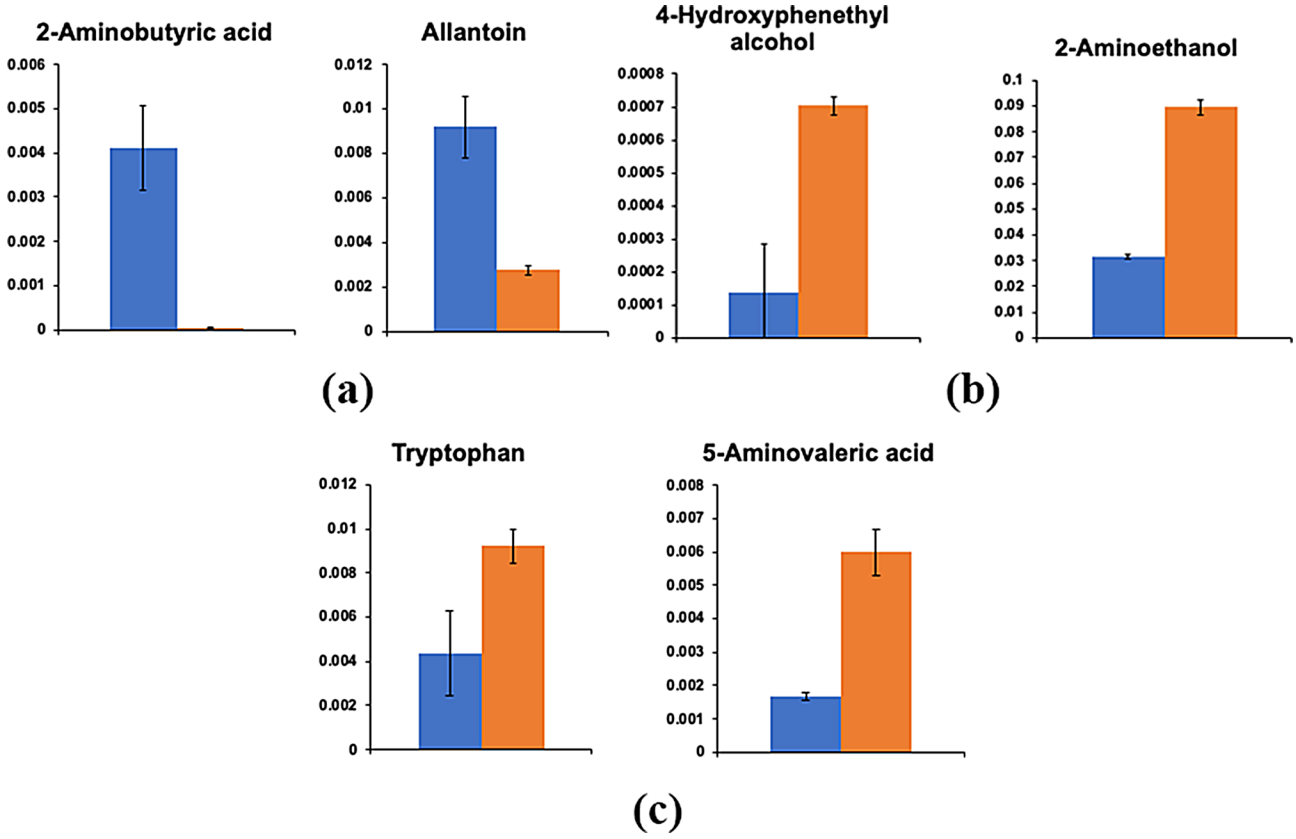

Fig. 7 Relative quantification of significantly correlated metabolites performed by GC/MS of DALE-22 (blue) and WT (orange). (**a**) Stress response and protective molecules. (**b**) Osmolytes and cellular water balance. (**c**) Amino acid breakdown and by-products. The data displayed represents the average of three biological replicate samples, with error bars showing the standard deviation from the mean

synthesis. The breakdown of it can occur through many pathways, which are determined by the specific requirements of the cell and the presence of certain enzymes. Insufficient breakdown of tryptophan can produce metabolites that may become poisonous when present in high doses. A cell with a more optimized mechanism to utilize or remove these byproducts may exhibit enhanced tolerance [32]. It indicates that the evolved strain, DALE-22, may have developed a better ability to utilize tryptophan in the presence of syringaldehyde compared to the parental strain. 5-amino valeric acid is generated through the degradation of several amino acids, such as glutamate and lysine. Like the by-products of tryptophan, the buildup of these substances can be poisonous. Cells that have a higher tolerance, such as DALE-22, may exhibit enhanced enzymatic activity for metabolizing or exporting these intermediates [33].

Conclusions

Flask-scale adaptive laboratory evolution (ALE) was utilized in this study to acquire a new strain of *Lipomyces starkeyi*, referred to as DALE-22, following 81 days of sequential fermentation. The findings demonstrated that the oleaginous yeast *L. starkeyi* DALE-22 exhibited superior bioconversion capability, cell proliferation, and generation of syringyl alcohol and lipids compared to the WT strain, which is referred to as the parental strain. This enhanced performance was observed specifically when exposed to syringaldehyde concentrations of up to 22 mM. On the other hand, WT was only able to utilize 4 mM syringaldehyde, given that DALE-22 has a superior phenotype compared to WT. The higher conversion capacity of DALE-22 also benefits the production of lipids as another by-product. The DALE-22 exhibits a notably enhanced ability to metabolize 22 mM syringaldehyde, leading to the efficient production of both syringyl alcohol and lipids. This finding is significant as it highlights *L. starkeyi's* potential for biotechnological applications, particularly in the valorization of lignin-derived compounds. When compared with existing literature, the efficiency of DALE-22 in utilizing syringaldehyde surpasses that of other potential yeasts previously reported. Juanssilfero et al. reported *L. starkeyi* NBRC10381 utilized 0.08 mM of syringaldehyde [34]. Other oleaginous yeast, such as *Tricosporon cutaneum* has the ability to effectively convert 0.75 mM syringaldehyde to another lignin derivative, including syringyl alcohol and syringic acid, with no accumulation of lipid produced [35]. For instance, earlier studies have documented lower conversion capacity and less effective lipid accumulation in similar conditions. The limitation of harnessing ALE in this study could be addressed in the future by implementing gene expression or metabolic engineering. An untargeted metabolomics analysis was conducted to investigate the regulation of compounds and identify crucial metabolites that may play a significant role in the cells during the bioconversion of lignin monomeric aldehydes, specifically syringaldehyde. Six significant metabolites associated with cell tolerance in the DALE-22 were discovered. This discovery could provide valuable insights for future advancements in cell development, potentially leading to even greater bioconversion capabilities. In summary, our work showcased the encouraging capability of ALE in enhancing the performance of *L. starkeyi* DALE-22 by increasing its tolerance and bioconversion capacity. This work also gives crucial insights into the metabolites that have potential benefits for cell development and shows excellent prospects for future uses in biorefinery.

Supplementary Information

The online version contains supplementary material available at https://doi.org/10.1186/s12934-024-02542-7.

Supplementary Material 1

Acknowledgements

We acknowledge the Ministry of Education, Culture, Sports, Science, and Technology (MEXT), Japan, for supporting the research. The New Energy and Industrial Technology Development Organization (NEDO) Feasibility Study Program, Japan, Grant Number JPNP14004, provided some funding for this work. This work was also financially supported by the International Joint Program, Science and Technology Research Partnership for Sustainable Development (SATREPS) from the Japan Science and Technology Agency and the Japan International Cooperation Agency (JST and JICA).

Author contributions

FJNP: conceptualization, data curation, formal analysis, methodology, validation, and writing-original draft; PK: editing, supervision, and writing review; AK and CO: resources and supervision. Each author has reviewed and consented to the manuscript.

Funding

This work was supported by The New Energy and Industrial Technology Development Organization (NEDO) Feasibility Study Program, Japan, Grant Number JPNP14004, which provided some funding for this work. This work was also financially supported by the International Joint Program, Science and Technology Research Partnership for Sustainable Development (SATREPS) from the Japan Science and Technology Agency and the Japan International Cooperation Agency (JST and JICA).

Data availability

No datasets were generated or analysed during the current study.

Declarations

Ethics approval and consent to participate

Not applicable.

Consent for publication

All authors approved the manuscript.

Competing interests

The authors declare no competing interests.

Received: 16 July 2024 / Accepted: 27 September 2024
Published online: 08 October 2024

References

1. Chauhan PS, Agrawal R, satlewal A, Kumar R, Gupta RP, Ramakumar SSV. Next generation applications of lignin derived commodity products, their life cycle, techno-economics and societal analysis. Int J Biol Macromol. 2022;197:179–200.
2. Wenger J, Haas V, Stern T. Why can we make anything from Lignin except Money? Towards a broader economic perspective in Lignin Research. Curr Forestry Rep. 2020;6:294–308.
3. Chettri D, Ahmed S, Malik AA, Verma AK. Lignin depolymerization for its valorization. Bioenergy Res. 2023.
4. Putra FJN, Kahar P, Kondo A, Ogino C. Valorization of Lignin and its derivatives using yeast. Processes. 2022;10:2004.
5. Pollegioni L, Tonin F, Rosini E. Lignin-degrading enzymes. FEBS J. 2015;282:1190–213.
6. Liu Q, Luo L, Zheng L. Lignins: Biosynthesis and Biological functions in plants. Int J Mol Sci. 2018;19:335.
7. Putra FJN, Kahar P, Kondo A, Ogino C. The bioconversion of lignin derivative aldehydes into high-value aromatic alcohols and lipids via *Lipomyces Starkeyi*. Biochem Eng J. 2023;200:109065.
8. Putra FJN, Kahar P, Kondo A, Ogino C. Production of lignin monomeric alcohols and lipids from oil palm empty fruit bunch by a combination of alkaline nitrobenzene depolymerization and *Lipomyces Starkeyi* bioconversion. Biochem Eng J. 2024;208:109347.
9. Lee S, Kim P. Current status and applications of adaptive laboratory evolution in industrial microorganisms. J Microbiol Biotechnol. 2020;30:793–803.
10. Halle L, Hollmann N, Tenhaef N, Mbengi L, Glitz C, Wiechert W, et al. Robotic workflows for automated long-term adaptive laboratory evolution: improving ethanol utilization by *Corynebacterium glutamicum*. Microb Cell Fact. 2023;22:175.
11. Saengphing T, Sattayawat P, Kalawil T, Suwannarach N, Kumla J, Yamada M, et al. Improving furfural tolerance in a xylose-fermenting yeast *Spathaspora Passalidarum* CMUWF1–2 via adaptive laboratory evolution. Microb Cell Fact. 2024;23:80.
12. Dragosits M, Mattanovich D. Adaptive laboratory evolution – principles and applications for biotechnology. Microb Cell Fact. 2013;12:64.
13. Kahar P, Itomi A, Tsuboi H, Ishizaki M, Yasuda M, Kihira C, et al. The flocculant *Saccharomyces cerevisiae* strain gains robustness via alteration of the cell wall hydrophobicity. Metab Eng. 2022;72:82–96.
14. Amza RL, Kahar P, Juanssilfero AB, Miyamoto N, Otsuka H, Kihira C et al. High cell density cultivation of *Lipomyces starkeyi* for achieving highly efficient lipid production from sugar under low C/N ratio. Biochem Eng J [Internet]. 2019;149:107236. https://linkinghub.elsevier.com/retrieve/pii/S1369703X19301639
15. Folch J, Lees M, Stanley GHS. A simple method for the isolation and purification of total lipides from animal tissues. J Biol Chem. 1957;226:497–509.
16. Nusantara Putra FJ, Putri SP, Fukusaki E. Metabolomics-based profiling of three terminal alkene-producing *Jeotgalicoccus* spp. during different growth phase. J Biosci Bioeng. 2019;127:52–8.
17. Jalu Nusantara Putra F, Kahar P, Ogino C, Kondo A. Advanced lignin valorization for biorefinery application. Advanced Lignin Technologies. IntechOpen; 2024.
18. Lyu L, Chu Y, Zhang S, Zhang Y, Huang Q, Wang S et al. Engineering the oleaginous yeast *Rhodosporidium toruloides* for improved resistance against inhibitors in biomass hydrolysates. Front Bioeng Biotechnol. 2021;9.
19. Postaru M, Tucaliuc A, Cascaval D, Galaction A-I. Cellular stress impact on yeast activity in biotechnological Processes—A short overview. Microorganisms. 2023;11:2522.
20. Zalomaeva OV, Podyacheva OYu, Suboch AN, Kibis LS, Kholdeeva OA. Aerobic oxidation of syringyl alcohol over N-doped carbon nanotubes. Appl Catal Gen. 2022;629:118424.
21. Abeln F, Chuck CJ. The history, state of the art and future prospects for oleaginous yeast research. Microb Cell Fact. 2021;20:221.
22. Tapia VE, Anschau A, Coradini AL, Franco T, Deckmann T. Optimization of lipid production by the oleaginous yeast *Lipomyces starkeyi* by random mutagenesis coupled to cerulenin screening. AMB Express. 2012;2:64.
23. Mindrebo JT, Patel A, Kim WE, Davis TD, Chen A, Bartholow TG, et al. Gating mechanism of elongating β-ketoacyl-ACP synthases. Nat Commun. 2020;11:1727.
24. Sun M, Shi Z, Zhang C, Zhang Y, Zhang S, Luo G. Novel long-chain fatty acid (LCFA)-degrading bacteria and pathways in anaerobic digestion promoted by hydrochar as revealed by genome-centric metatranscriptomics analysis. Appl Environ Microbiol. 2022;88.
25. Yagin F, Alkhateeb A, Colak C, Azzeh M, Yagin B, Rueda L. A fecal-microbial-extracellular-vesicles-based metabolomics machine learning framework and biomarker discovery for predicting colorectal cancer patients. Metabolites. 2023;13:589.
26. Cui Y, Miao K, Niyaphorn S, Qu X. Production of gamma-aminobutyric acid from lactic acid bacteria: a systematic review. Int J Mol Sci. 2020;21.
27. Wu Q, Su N, Huang X, Cui J, Shabala L, Zhou M, et al. Hypoxia-induced increase in GABA content is essential for restoration of membrane potential and preventing ROS-induced disturbance to ion homeostasis. Plant Commun. 2021;2:100188.
28. Raihan MRH, Rahman M, Rastogi A, Fujita M, Hasanuzzaman M. Exogenous Allantoin confers rapeseed (*Brassica campestris*) tolerance to simulated drought by improving antioxidant metabolism and physiology. Antioxidants. 2023;12:1508.
29. Bernini R, Carastro I, Santoni F, Clemente M. Synthesis of lipophilic esters of tyrosol, homovanillyl alcohol and hydroxytyrosol. Antioxidants. 2019;8:174.
30. Belda I, Ruiz J, Esteban-Fernández A, Navascués E, Marquina D, Santos A, et al. Microbial contribution to wine aroma and its intended use for wine quality improvement. Molecules. 2017;22:189.
31. Krysenko S, Wohlleben W. Polyamine and ethanolamine metabolism in Bacteria as an important component of nitrogen assimilation for survival and pathogenicity. Med Sci. 2022;10:40.
32. Shaw C, Hess M, Weimer BC. Microbial-derived tryptophan metabolites and their role in neurological disease: Anthranilic Acid and Anthranilic acid derivatives. Microorganisms. 2023;11:1825.
33. Sasikumar K, Hannibal S, Wendisch VF, Nampoothiri KM. Production of biopolyamide precursors 5-Amino valeric acid and putrescine from rice straw hydrolysate by engineered *Corynebacterium glutamicum*. Front Bioeng Biotechnol. 2021;9.
34. Juanssilfero AB, Kahar P, Amza RL, Miyamoto N, Otsuka H, Matsumoto H, et al. Selection of oleaginous yeasts capable of high lipid accumulation during challenges from inhibitory chemical compounds. Biochem Eng J. 2018;137:182–91.
35. Hu M, Wang J, Gao Q, Bao J. Converting lignin derived phenolic aldehydes into microbial lipid by *Trichosporon Cutaneum*. J Biotechnol. 2018;281:81–6.

Publisher's note